Fire Safety Journal **20** (1993) 203–225

Effects of Sample Mounting on Flammability Properties of Intumescent Polymers†

Takashi Kashiwagi & Thomas G. Cleary

Building and Fire Research Laboratory, National Institute of Standards and Technology, Gaithersburg, Maryland 20899, USA

(Received 25 July 1991; revised version received 25 December 1991; accepted 7 January 1992)

ABSTRACT

Various flammability properties of polycarbonate samples were measured with the cone calorimeter and lateral ignition and flame spread (LIFT) devices at various external fluxes. Four different sample mountings were used with the cone calorimeter to investigate the effects of sample mounting on the flammability properties of these samples. One sample mounting configuration employed the standard metal edge frame and a grid to retain intumesced char. The other three sample mounting configurations allowed the intumesced char to rise free. The results show that peak heat release rates and heat release rate curves were significantly affected by the sample mounting configuration but total heat released, effective heat of combustion, and soot yield were not significantly affected. Flame spread characteristics were measured with the LIFT. Two sample mounting configurations were used, the standard method and the standard method with the addition of a wire grid to retain intumesced char. Significant differences in flame spread rates were observed between the two sample mounting configurations with and without the grid. This was caused by differences in flame spread rates versus rising rates of char.

1 INTRODUCTION

For prediction of fire growth hazard involving polymeric materials, it is important to measure various flammability properties, for example,

† Contribution from the National Institute of Standards and Technology, not subject to copyright.

Fire Safety Journal, Vol. 20, No. 3, 203-225, 1993. Interscience Communications Limited. Heat Release and Fire Hazard. 1st U. S. Symposium. Abstracts. December 1991, San Diego, CA, 4 pp, 1991.

ignition delay times, flame spread rates, heat release rates, smoke and carbon monoxide (CO) yields, and so on. These properties are measured by various bench-scale tests. The measured results are used as input data to a mathematical model for predicting the behavior of material in a fire.[1] This new approach allows for the assessment of the fire hazard of a polymer sample in various applications instead of the more traditional approach of using a screening test at a specified set of conditions. Thus, this approach can provide definitive information for a plastic manufacturer regarding the fire performance of his products and the effectiveness of a specific flame retardant treatment for a range of end-use applications.

There are two bench-scale tests which can measure the flammability properties described above: the cone calorimeter[2] and the lateral ignition and flame spread device[3] (LIFT). The former measures ignition delay time, heat release rate, CO and soot yields, and the latter measures opposed-flow flame spread characteristics. During the combustion of most engineering polymers char is formed and often the char intumesces. Intumesced char can interfere with the measurement of flammability properties, typically by distorting the surface and rising upward, such that the radiant flux on the sample surface from an external source is no longer well defined. In some configurations intumesced char can also block radiation. In order to avoid the interference caused by intumesced char, commonly a grid or a wire screen has been used to hold down the char. However, it is expected that some degree of char intumescence would occur for these samples in a real fire. Therefore, it is not clear whether the measured results with the grid or the screen truly represent real-world flammability properties of intumescent materials. The objective of this study is to (i) identify what flammability properties of intumescent polymers are affected by sample mounting, (ii) investigate how sensitive they are to mounting, and (iii) determine whether sample mounting impacts the measured effectiveness of fire retardant treatment on flammability properties.

2 EXPERIMENTAL DESCRIPTION

2.1 Materials

Two different types of polymer samples were used; one was a polycarbonate (PC) and the second was a ULTEM$^{\circ R2}$polyetherimide (PEI). All polymer samples were supplied by General Electric Co.

Base samples with the least amount of additives of the given polymer type were designated as PC A and PEI A. Several flame retardant treated samples were also included for both polymer types and they were designated as PC B and PC C for polycarbonate and as PEI B and PEI C for polyetherimide. The thickness of all samples was approximately 0·3 cm.

2.2 Measurement methods of flammability properties

Two bench-scale test methods—the cone calorimeter[2] and a modified LIFT[3]—were used in this study. Both devices were built at NIST. The sample size for the cone calorimeter experiments was approximately 10 × 10 cm and that for the LIFT experiments was approximately 16 cm in width ×80 cm in length. A horizontal sample orientation was used for cone calorimeter experiments. The normal sample orientation for the LIFT is vertical, which posed a problem for materials that can melt and drip out of the sample holder. To overcome this problem for the materials examined here (all samples used in this study melt and drip in the LIFT apparatus), the LIFT was rotated 90° such that the sample was horizontal with the radiant heat source located above the sample (HIFT configuration). Flame spread in this orientation is still characterized as opposed flow in nature and the HIFT configuration is assumed to be nearly equivalent to the LIFT arrangement. For the ignition tests an air–acetylene pilot flame extended over the sample from one edge to the center of the sample at a height of approximately 3 cm above the sample. The horizontal orientation poses some problems for the flame spread tests. Once a sample is burning, flame may heat up the radiant panel and radiation from the flames may contribute to the sample surface preheating beyond the flame front. These effects and attenuation of the radiation from the panel by smoke emitted from a burning sample were determined by continuous measurement of radiant flux at a location near the end of the sample during a test. The results show that momentary increases of up to 40% in radiant flux or up to 10% decrease by smoke obscuration are observed. However, this momentary change in radiant flux appears to be a secondary effect and will be ignored in this study.

2.3 Different sample mounting methods

Intumescent samples are generally tested in the cone calorimeter using a screen/grid directly over the irradiated sample surface to suppress the intumescing char and to keep the sample surface at the initial location

relative to the cone heater element. A metal edge frame is generally used to mount the screen/grid. Here, the aluminum foil was used to wrap the sides and bottom of the sample and various screens with differing mesh sizes were used on the sample surface to hold down the intumescing char; they were generally very close to the irradiated sample surface. However, all the attempts failed to hold down the char. The molten polymer layer seeped through the screen/grid during the pre-ignition period even with a fine mesh screen and intumescent char was formed above the screen/grid. (The char mound reached to the heater element during the burning period. This behavior is similar to

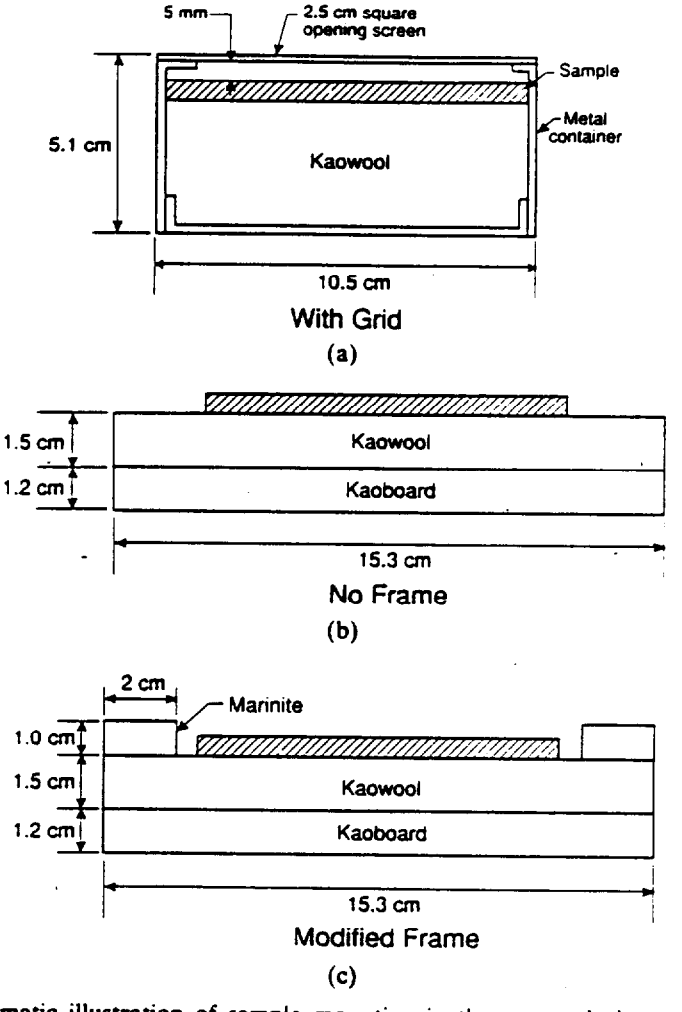

Fig. 1. Schematic illustration of sample mounting in the cone calorimeter, (a) WG configuration, (b) NF configuration, and (c) MF configuration.

the sample mounting configuration with the metal frame without the grid noted as NG in this paper.) Based on this observation and several trial tests, a coarse screen/grid of about 2·5 cm square opening was installed at 0·5 cm above the initial sample surface location to hold down the intumesced char after it had solidified. Interference from the coarse screen/grid appeared to be negligible for the measured flame properties and any changes in radiant flux received at the sample surface due to 0·5 cm upward shift of the sample surface from the initial location were negligible. A schematic illustration of the final sample holder configuration is shown in Fig. 1(a). This configuration was denoted as being with the screen/grid and the metal container and is here abbreviated, WG. One of the three additional configurations was without the screen/grid but with the metal container, denoted as being the no grid configuration, NG. The other two configurations used neither the screen/grid nor the metal edge frame. In one configuration a sample was placed on a Kaowool slab without any frame as shown in Fig. 1(b) and denoted as being the no frame configuration, NF. The last one was similar to NF but with a non-metallic frame to contain potential polymer melt flow and this was denoted as the modified frame configuration, MF, and is shown in Fig. 1(c). All sides of a sample were covered by a thin aluminum foil except the front surface.

For the HIFT experiments two sample mounting configurations were used: one was with a coarse wire screen (chicken wire) covering the sample surface to hold down intumesced char and the other was without the wire.

3 RESULTS

3.1 Flammability properties measured by cone calorimeter

3.1.1 *Behavior of intumesced char*

With the three configurations without the screen/grid, i.e. NG, NF and MF, the intumesced char was not restricted nor was the sample height adjusted to maintain a constant distance to the cone heater element. Sometimes the intumescing char rose to touch the cone heating element or rose further and came through the opening of the cone heater element. Generally, an intumesced char tends to a maximum height with the NG configuration (without the screen/grid but with the metal edge frame). In this configuration, the center of the sample charred. Because of heat losses to the metal edge frame, the sample in contact with the metal edge frame did not char but melted. Gaseous degrada-

tion products beneath the sample surface could not efficiently escape from the sample sides which were sealed by the melting polymer touching the cooler metal wall. The accumulation of gaseous degradation products below the sample surface pushed the central part of the charred sample upward. Continuation of this process generated a high-rising char mound which sometimes touched the cone heater element or went through the opening of the cone. Char mounds which did not rise as high were observed with the NF configuration and the MF configuration which did not use the metal edge frame. Gaseous degradation products appeared to escape more easily from the sample along the four sides. Some slow outward flowing movement of melting polymer was occasionally observed with the NF configuration. Generally, char mounds of burning polycarbonate samples, except in the WG configuration, tended to rise higher than those of PEI samples. When char mounds touched the cone heater element, abnormalities such as an apparent weight gain were observed.

3.1.2 *Repeatability*

Repeatability of the test results was examined and the results for the heat release rate are shown in Fig. 2 for two different samples. The heat release rate for PEI A was measured in the WG configuration and the NF configuration was used for PC A. The piloted ignition delay time

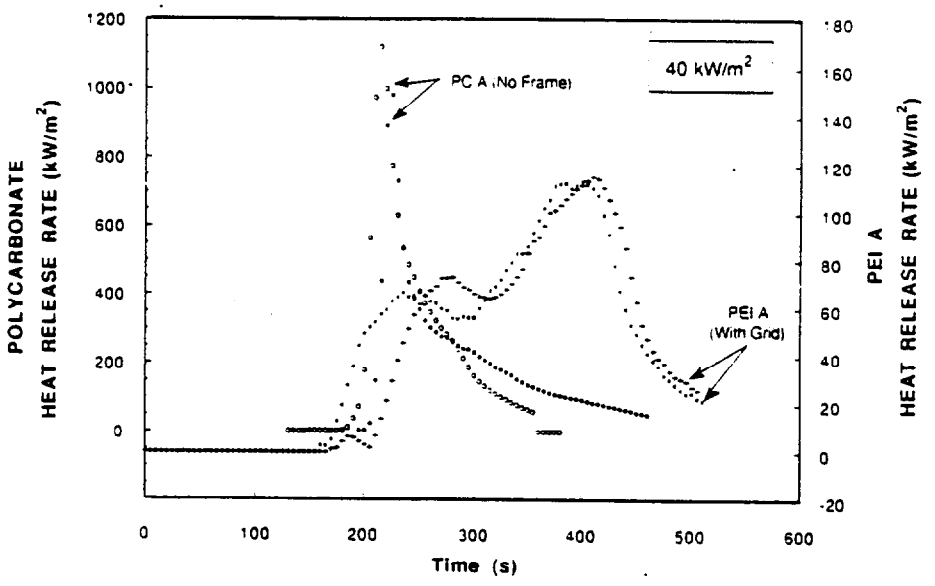

Fig. 2. Repeatability of heat release rate of PC A and PEI A at an external flux of 40 kW/m².

determined in the cone calorimeter for the polymer samples used in this study tends to be less repeatable that non-intumescent polymer materials due to (i) localized outgassing of gaseous degradation products by a rupture in the char or polymer melt layer, which often caused localized ignition upon gas contact with the cone heater element; and (ii) a rapid rise of the char mound which changed the external radiant flux to the sample surface and which also requires movement of the spark pilot away from its initial location. Therefore, as seen in Fig. 2, scatter in the times to ignition caused the heat release rates curves to be offset from each other for the repeat tests. However, the repeatability of the overall heat release rate curve is adequate for the present study. Therefore, two tests were repeated for each test condition unless there was large discrepancy between the results between the two tests. For the rapid increase in heat release rate observed with PC A, the standard instrument scanning rate of 1 scan/5 s for the cone calorimeter might not be fast enough to determine the peak heat release rate accurately. The response times of the oxygen analyzer and the flow system are also important in accurately determining the peak heat release rate.

3.1.3 *Flammability properties*

Heat release rates of PC A in the four different sample mounting configurations were measured at an external radiant flux of 40 kW/m^2; their comparison is shown in Fig. 3. As described above, since the

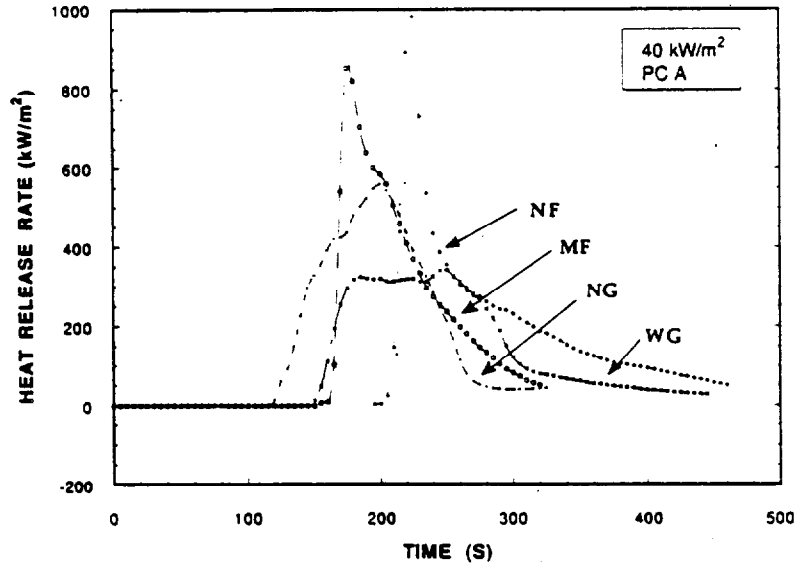

Fig. 3. Effects of sample mounting on heat release rate of PC at 40 kW/m^2.

ignition event was rather irregular without the screen/grid, the differences in ignition delay time among the four different sample mounting configurations may not be significant. The results show a clear trend in the heat release rate curves for different sample mounting configurations. In the WG configuration (char was held down by the screen/grid) the heat release rate is generally lower than those in the three configurations with char mounds. Shortly after ignition, a very large flame was observed visually in the NF and MF configurations followed by a small flame anchored at the top part of the char mound. Correspondingly, large peak heat release rates were generated in these two configurations, as shown in Fig. 4. However, total heat released varied only by about 10% with the four different configurations, as shown in Fig. 5. The samples lost about 70% of their initial weight and the effective heat of combustion was nearly the same for the four configurations, as shown in Fig. 6. Soot yield was measured by weighing particulates collected on a filter from a fraction of the exhaust gas; the result is shown in Fig. 7. Again there is no significant effect of sample mounting on soot yield (within 10% change). For time-integrated values no significant effects of sample mounting on flammability properties of PC A were observed (The CO yield and average specific extinction area, which are not shown in this paper due to space restrictions, were not significantly affected by sample mounting.)

A similar trend was also observed for a PEI A sample; the effects of

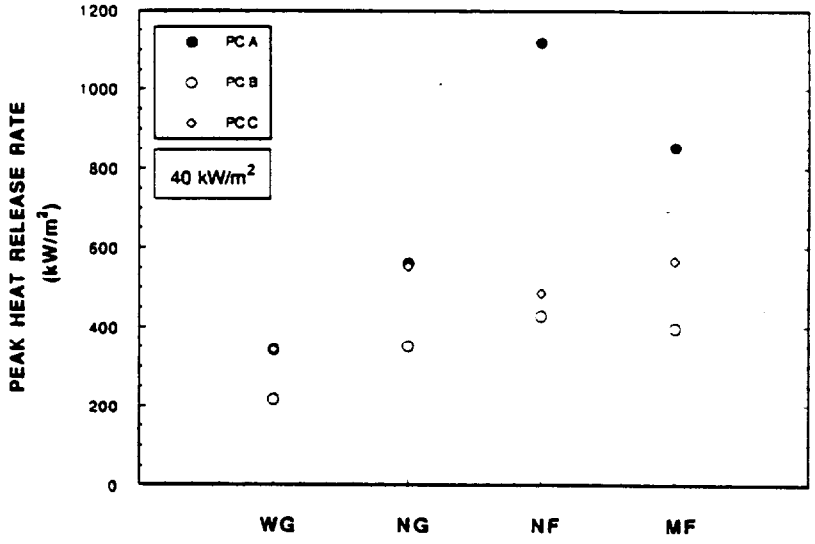

Fig. 4. Effects of sample mounting on peak heat release rate of polycarbonates at 40 kW/m^2.

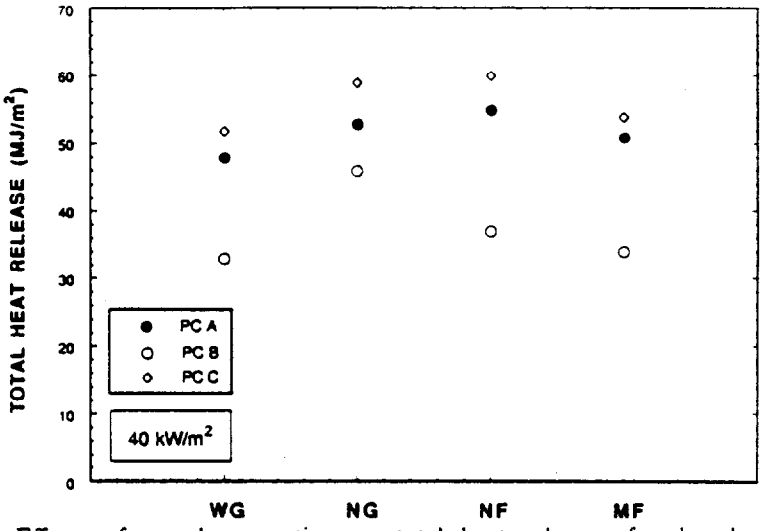

Fig. 5. Effects of sample mounting on total heat release of polycarbonates at 40 kW/m^2.

sample mounting on heat release rate of a PEI A sample are shown in Fig. 8. The finding of a high peak heat release rate at the beginning of burning in the NF and MF configurations is the same as that for a PC A sample. Peak heat release rate, total heat release, and total sample weight loss of a PEI A sample increased from the WG and NG

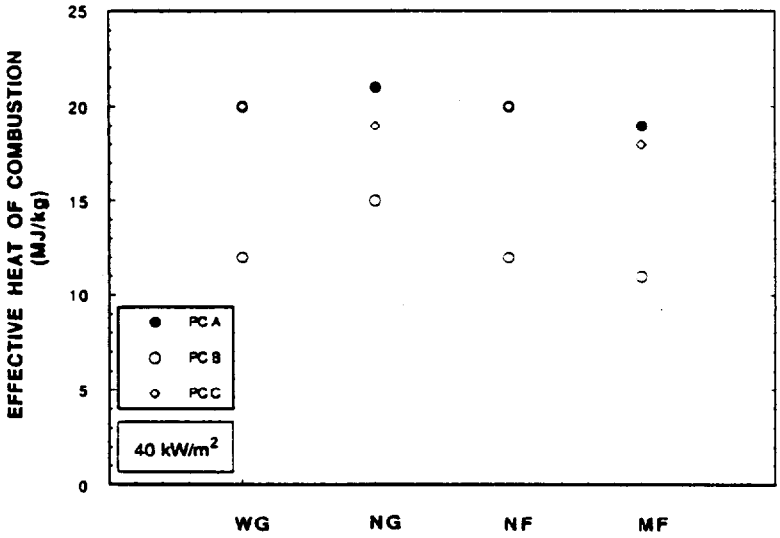

Fig. 6. Effects of sample mounting on effective heat of combustion of polycarbonates at 40 kW/m^2.

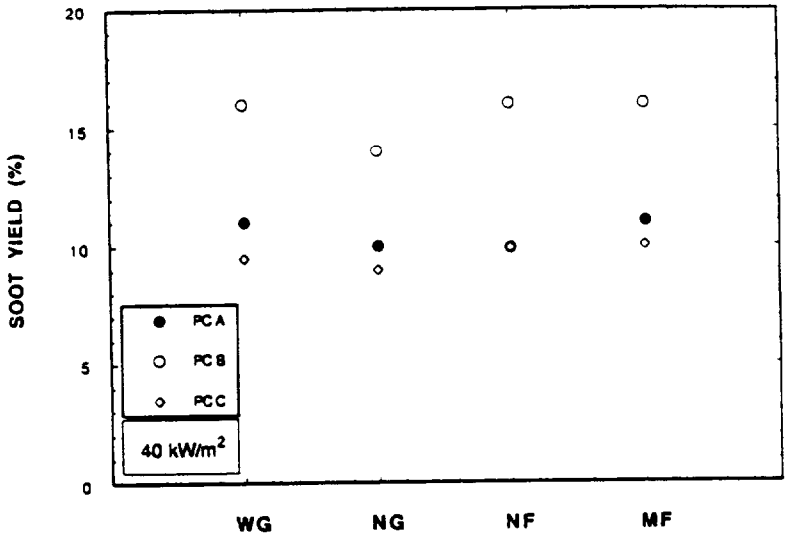

Fig. 7. Effects of sample mounting on soot yield of polycarbonates at 40 kW/m^2.

configurations to the NF and MF configurations. The increase in peak heat release rate between these two sets of data was approximately 100%. A comparison of total sample weight loss and total heat release showed about a 30% increase. However, effective heat of combustion and soot yield of a PEI A sample were not significantly affected by sample mounting configuration.

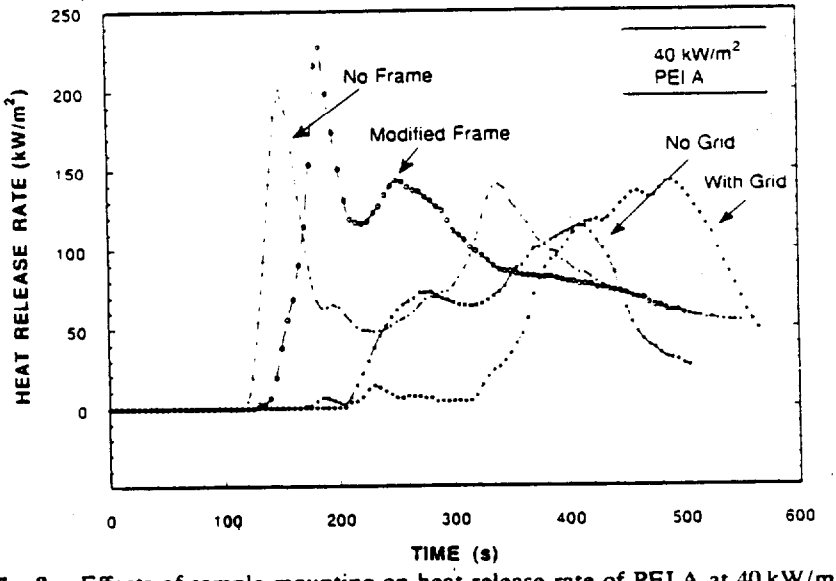

Fig. 8. Effects of sample mounting on heat release rate of PEI A at 40 kW/m^2.

The effects of sample mounting on the effectiveness of flame retardant treatment were determined by comparing flammability results of flame retardant treated PC B and PC C samples to those of PC A sample in the four different sample mounting configurations. The peak heat release rate of flame retardant treated PC B and PC C samples did increase in the NF and MF configurations relative to the NG and WG configurations. However, the amount of the increase for PC B and PC C was much less than for PC A, as shown in Fig. 4; their peak heat release rates were still lower or at least equal to those for PC A. Therefore, the order of effectiveness of the flame retardant treatments did not change with differences in sample mounting configuration. Total heat released, effective heat of combustion, and soot yield for the flame retardant treated PC samples were not significantly affected by sample mounting and, furthermore, the quantitative effectiveness of flame retardant treatment was not significantly altered by sample mounting as shown in Figs 5–7.

The effects of sample mounting on the effectiveness of flame retardant treatment for PEI B and C samples were also studied. The results indicate that the peak heat release of these samples was not significantly affected by sample mounting. (These samples did not intumesce as high as the PC samples.) There were no significant effects of sample mounting on effective heat of combustion, soot yield, total heat released and total sample weight loss of the flame retardant treated PEI samples. Therefore, the order of effectiveness of the flame retardant treatment for the PEI samples was not significantly altered by sample mounting.

3.2 Flame spread characteristics measured by HIFT

3.2.1 *Flame spread behavior*

The time histories of the flame front position for a PC A sample with and without the grid (chicken wire) are plotted in Fig. 9. The highest external flux at one end of the sample was set at 40 kW/m^2 and the sample was preheated for 180 s. This preheating time was selected to provide a long enough preheating without significant charring of the sample and also without ignition caused by the contact of degradation products with the hot gas-fired radiant panel. The results show that flame spread rapidly in the high external radiation region, near the location of piloted ignition, and the flame spread rate (slope of the curve shown in Fig. 9) gradually decreased as the flame front moved toward lower external radiant flux region. There were no significant differences in flame spread rate with and without the grid. A curled-up char layer was formed long after the passage of the flame front without

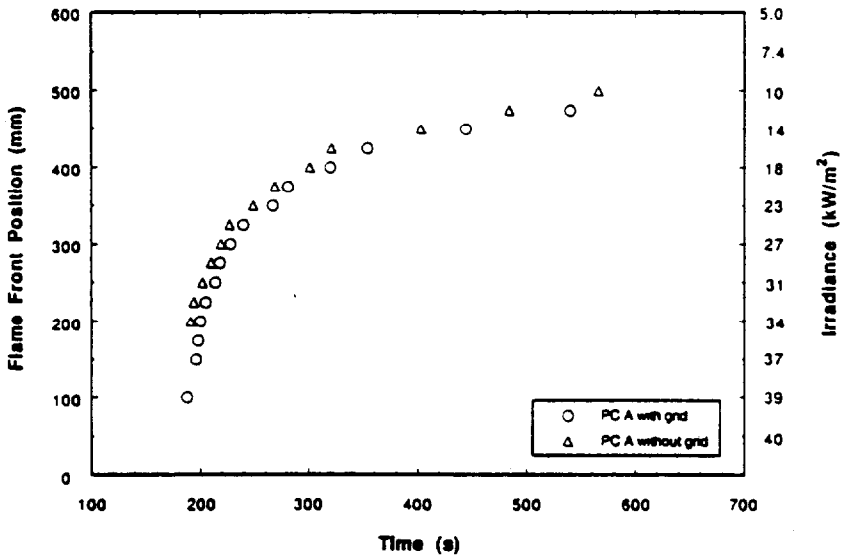

Fig. 9. Comparison of history of flame front spreading over PC A surface in the configurations with and without a grid.

the grid. Therefore, the flame spread over a nearly flat surface before the char mound was fully formed.

When a PEI A sample was tested without the grid, the final charred and intumesced sample took on the appearance of the top half of a loaf of bread; it was highest (about 6 cm) at the center of the sample, and lowest at the sides of the sample which were clamped by the metal frame. Since the flame spread rate was not fast enough for the flame front to travel well-ahead of the rising char mound, flame spread was significantly affected by the char mound. Sometimes flames spread along the sides close to the metal edge frame, where the sample was not well charred due to heat losses to the metal edge frame. Generally, the flame appeared to be sporadic and localized, dependent on the supply of evolved degradation products through some opening in the char mound, instead of forming a near one-dimensional flame front as observed with the grid. A comparison of the results with and without the grid is shown in Fig. 10. Although the results without the grid were not highly reproducible, flame spread was generally much slower and required more external flux to sustain flame spread than with the grid. This was possibly caused by reduction in external radiant flux reaching the sample surface ahead of the mound due to blocking of the radiation by the mound.

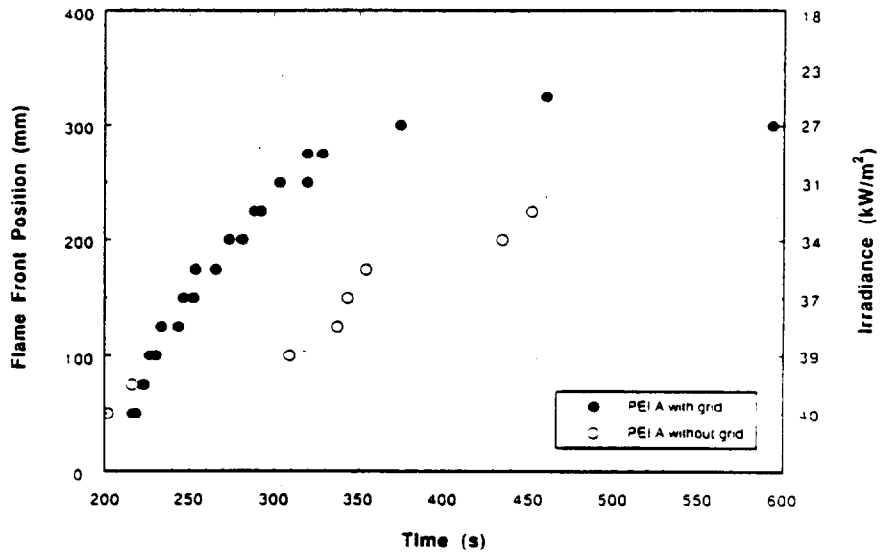

Fig. 10. Comparison of history of flame front spreading over PEI A surface with and without a grid.

3.2.2 *Flame spread properties*

In this section, a derivation of material flammability properties is briefly described. The material flammability properties and the heat release rate curve measured by the cone calorimeter are used in the prediction of upward flame spread on a wall in a later part of this paper. Ignition and opposed flow flame spread data can be presented in flammability diagrams which graphically display both the data and a model fit for each material.[4] This approach was applied to the measured flame spread data for PC A and PEI A samples. The flammability diagram for PC A with grid is shown in Fig. 11. Similar results for PEI A are not shown due to space limitations. The left ordinate gives the flame spread rate, the right ordinate gives the time to piloted ignition, and the abscissa is external radiant flux.

One of the solid lines in Fig. 11 is the correlation of piloted ignition delay time, t_{ig}, with external radiant flux, $\dot{q}''_e$, based on a one-dimensional semi-infinite inert heat conduction model. The model expression is given by[5]

$$t_{ig} = \pi k\rho c(T_{ig} - T_0)^2/(4\dot{q}''^2_e) \tag{1}$$

where T_{ig} is an inferred sample surface temperature at ignition, T_0 is the initial sample temperature, $k\rho c$ is an effective thermal inertia (product of thermal conductivity, density, and heat capacity of the material) over

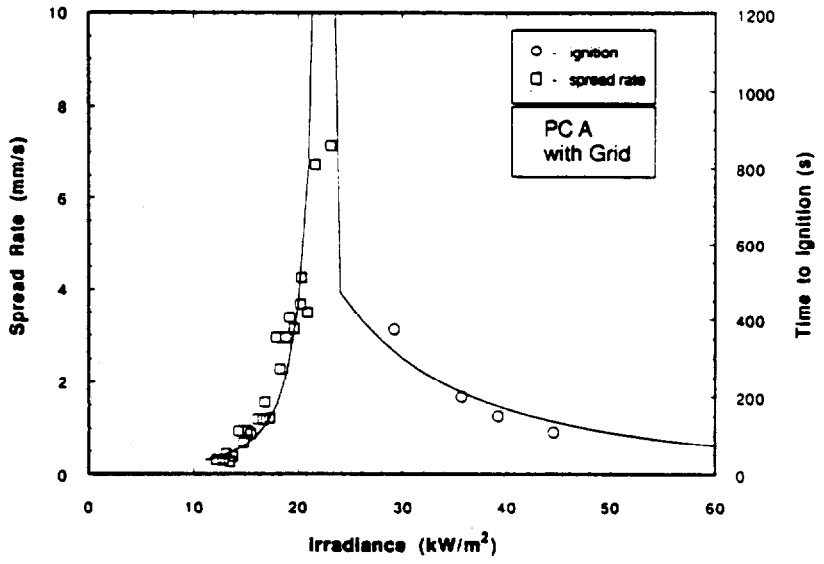

Fig. 11. Flammability diagram of PC A with a grid consisting of piloted ignition and flame spread characteristic curve.

the temperature range from T_0 to T_{ig}, thus $k\rho c$ can be considered as one of the material's 'flammability properties'.

A semi-empirical opposed flow flame spread model predicts the flame spread rate, V, as[6]

$$V = \Phi/(k\rho c(T_{ig} - T_s)^2) \tag{2}$$

where Φ accounts for heat transfer from the flame to the unburned material ahead of the flame front. Φ depends somewhat on the test conditions, but it is approximately equivalent for lateral, downward, and horizontal spread under conditions of natural convection.[7] Material surface temperature ahead of the advancing flame front, T_s, is determined from the energy balance between the external incident flux, $\dot{q}''_e$, and losses by re-radiation and convection. A minimum external flux or material surface temperature for opposed flame spread was estimated from the flame spread test.

The other solid line for flame spread in Fig. 11 was obtained by the best fit of eqn (2) to the measured flame spread data, using the above derived values of T_{ig} and $k\rho c$. From the fit the value of Φ was determined. Since all piloted ignition tests using the HIFT configuration were conducted with a wire grid to eliminate the possibility of an intumescing char contacting the pilot flame, the same values of T_{ig} and $k\rho c$ were used for determination of Φ in the configuration without the

TABLE 1
Ignition and Flame Spread Properties

Material	$\dot{q}''_{ig}$ (kW/m^2)	T_{ig} $(°C)$	$k\rho c$ $(kW/m^2K)^2s$	Φ (kW^2/m^3)	$\dot{q}''_s, min$ (kW/m^2)
PC A	23	464	1·75	24·3	12
PC A[a]	—[b]	—	—	32·0	12
PC B	22	455	1·76	10·5	15
PEI A	28	507	2·72	71·7	24
PEI A[a]	—	—	—	140	32
PEI B	29	514	3·36	[c]	25
PEI C	30	524	2·45	[c]	25

[a] Without screen.
[b] Ignition data not taken.
[c] No data curve fit.

wire grid. A summary of the inferred ignition and flame spread parameters is given in Table 1. The notation $\dot{q}''_{ig}$ is the minimum external flux for piloted ignition. In Fig. 11 the flame spread rate data lie above some external radiant flux which signifies that the material exhibits a finite minimum external radiation flux for spead, $\dot{q}''_{s,min}$, and its value is listed in Table 1. The results indicate that there are significant effects of sample mounting on values of flammability parameters for PEI A but the effects are minor for PC A. The values of Φ measured for the PC samples on the HIFT are from 10 to 32 which are much larger than a typical value of Φ which is generally from 1 to 15 measured on the LIFT.[3] Since the flame spread study was conducted in the HIFT configuration, the luminous flame from the burning PC samples became tall enough to increase radiation feedback from the flame to the sample surface ahead of the flame front. This tends to increase the value of Φ. Generally, a flame retardant treatment tends to lower the value of Φ, which is seen for the PC B sample. Extremely large values of Φ for the PEI samples are probably due to applying the above model to intumesced samples over which flame spread was irregular and sporadic as discussed above.

4 DISCUSSION

The above results indicate that the sample mounting configuration significantly affects the heat release rate curve, particularly peak heat release rate. It does not affect as significantly other integrated pro-

perties such as total heat release, sample weight loss, soot yield, and effective heat of combustion. Without the grid and the metal edge frame for the cone calorimeter (NF and MF configurations), the heat release rate for PC and PEI samples increased much more rapidly shortly after ignition than comparable samples tested with the grid and the metal edge frame. This is probably due to an increase in exposed surface area generating more combustible degradation gaseous products and to an increase in absorbed external radiation because of the shorter distance between the heater element and the rising char mound. This is also supported by a more rapid increase in the heat release rate for the NG configuration (without the grid but with the metal edge frame) than for the WG configuration (with the grid and the metal edge frame). The metal container acts as a heat sink and the loss of energy to the metal container from the sample delays an increase in heat release rate.

After the initial surge of high heat release in the NF and MF configurations, heat release rate decreased rapidly probably due mostly to blocking of the external radiation by the char mound. Therefore, the effects of the char mound on heat release rate are very complicated. Clearly, the height of the char mound has a strong influence on the heat release rate. Unfortunately, the height of the char mound depends on the sample mounting configuration and also probably on the size of the sample. At present it is not clear which sample mounting configuration and sample size of sample represent a true measure of the flammability properties of the material which can be applied to predict its behavior in an actual fire.

In the HIFT experiment, clamping of the sample by the sample holder appeared to have a significant effect on the rise of the char mound. Once a char layer rises, resembling a loaf of bread, it is extremely difficult to analyze the data. This is due to the change in external flux distribution and non-one-dimensional sporadic flame front. It might be useful to study the effects of non-clamped sample edges and of larger sample size on flame spread characteristics.

Although it has been demonstrated here that some flammability properties are significantly affected by the sample mounting configuration in the bench-scale tests, it is important to find how much the calculated fire growth and heat release rate in a full-scale fire are affected by using the flammability properties measured by the different sample mounting configurations as inputs to a theoretical model. One particular fire scenario, fire growth up a wall, was selected as a demonstration. It was assumed that the wall was composed of the particular materials whose flammability properties were measured in this study, and was exposed to a small fire such as that in a waste-paper

basket. Then, the location of the pyrolysis front, y_p, can be expressed as[1]

$$\frac{dy_p}{dt} = \frac{y_f - y_p}{t_{ig}} \tag{3}$$

where y_f is the position of the flame tip with $y_f - y_p$ defining the forward heat transfer region of the flame with heat feedback flux, $\dot{q}''_f$, which is the average flame heat flux to the surface over the flame length. An approximation to flame tip height is given below:

$$y_f - y_b = k_f(\dot{Q}'_0 + \dot{Q}''_{avg}(y_p - y_b))$$

where y_b is the position of the burnout front, k_f is a constant, $\dot{Q}'_0$ is the ignitor strength per unit width, and $\dot{Q}''_{avg}$ is an average heat release rate per unit area of the pyrolyzing material. The ignition delay time can be calculated by eqn (1). The location of the burnout front, y_b, can be approximated as

$$\frac{dy_b}{dt} = \frac{y_p - y_b}{t_b} \tag{4}$$

where t_b is an effective burnout time. With appropriate initial and boundary conditions, including the average heat release rate of the ignition source, the solution to the above equations are given below:[1]

$$\frac{y_p}{y_0} = \frac{(a+1)}{a} e^{a\tau} - \frac{1}{a} \tag{5}$$

for $0 \le \tau \le t_b/t_{ig}$ where $\tau \equiv t/t_{ig}$ and $a = k_f \dot{Q}''_{avg} - 1$. y_0 is the initial pyrolysis length due to the ignition source needed to initiate the process, and $y_0 = k_f \dot{Q}'_0$. For $\tau > (t_b/t_{ig}) \equiv \tau_b$, the solutions are

$$\frac{y_p - y_b}{y_0} = c e^{b(\tau - \tau_b)} \tag{6}$$

$$\frac{y_b}{y_0} = 1 + \frac{c}{b\tau_b}(e^{b(\tau - \tau_b)} - 1) \tag{7}$$

where $b = a - 1/\tau_b$ and $c = (a+1)/a\,(e^{a\tau_b} - 1)$.

The parameters a and b must be greater than zero in order for the upward flame spread to accelerate. For values less than zero, the spread will eventually stop.

The above model does not include the effects of an enclosing compartment on the flame spread process; such effects include radiation feedback from the other walls to the burning wall or convective heating of the upper part of the wall from the hot upper layer. Also, melting

and dripping of the PC A and PEI A were ignored. Although these phenomena could have significant effects on upward flame spread, at present there is no theoretical model of flame spread which includes the behavior of melting and dripping of molten polymer layers. For the simulations a continuous 50 kW fire of waste-paper basket size was assumed to be the ignition source. A flame height of 0·5 m above the ignition source was estimated. The maximum pyrolysis height was set at 2·4 m which is the common ceiling height in a residential dwelling. The model calculates the pyrolysis area from the above equations for upward spread and the total rate of heat release per unit width was obtained by multipling this area by the average rate of heat release per unit area obtained from the cone calorimeter at 40 kW/m^2. The average rate of heat release was thus approximated by choosing as 90% of the peak rate of heat release value. Thus, the heat release rate curve was approximated as a square wave. The width of the square wave was determined by dividing the total heat release by this peak-average value (also t_b was thus determined). The width of this square wave was then considered as the effective burn time. The ignition delay time was also obtained at an external radiant flux of 40 kW/m^2. Although the average flame heat feedback flux to the non-pyrolyzing sample surface is typically in the range 25–30 kW/m^2 for the luminous portion of the flame,[8] the value of 40 kW/m^2 was selected. This flux may be representative of conditions achieved in a room fire or corner fire (in testing this model against experiment, Cleary and Quintiere[1] tried flammability properties measured by the cone calorimeter at external radiant flux of both 25 and 50 kW/m^2 from the Swedish room fire tests). The most important concept of this model is that energy feedback rate from the flame to the non-pyrolyzed sample surface is assumed to be a constant (in this study at 40 kW/m^2) during the upward flame spreading period but the preheating area increases with increasing flame height by flame spread.

The calculated growth of the pyrolysis height with time for PC A is shown in Fig. 12 using flammability data obtained from the sample mounting in the WG and MF configurations. Both results indicate that flame spreads to the top of the wall (2·4 m) and there is no appreciable difference in ignition delay time and the rate of flame spread calculated with the data in the MF configuration and in the WG configuration. The corresponding heat release rate per unit width of the wall is shown in Fig. 13. The results include the continuous 50 kW/m heat release rate from the ignition source throughout the calculation. Here the results show a significant difference in heat release rate. The data based on the MF configuration predicts roughly twice as large a peak heat

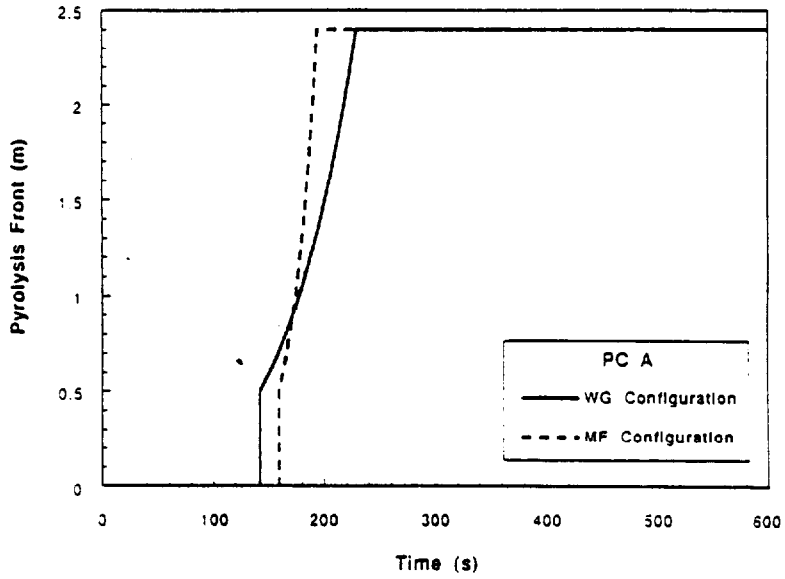

Fig. 12. Comparison of calculated growth of pyrolysis height for upward flame spread over PC A using flammability properties measured in the WG and MF configurations.

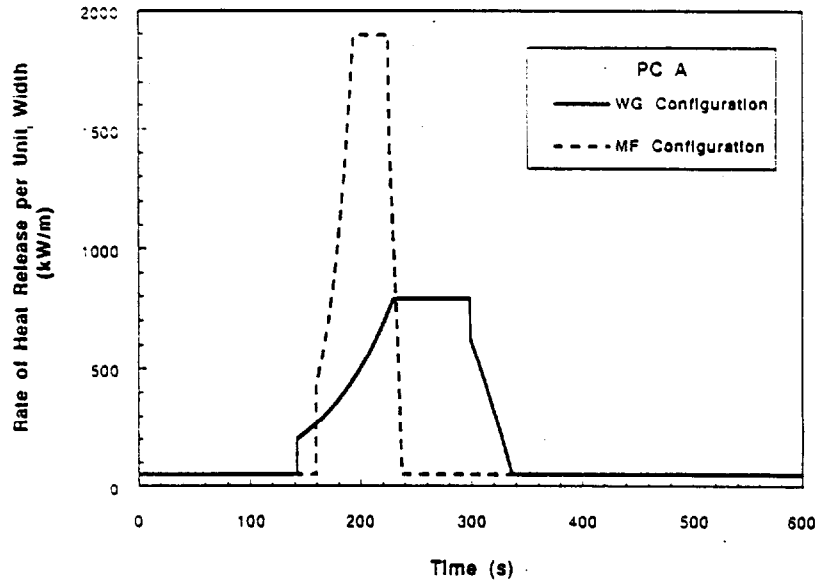

Fig. 13. Comparison of calculated heat release rate for upward flame spread over PC A using flammability properties measured in the WG and MF configurations.

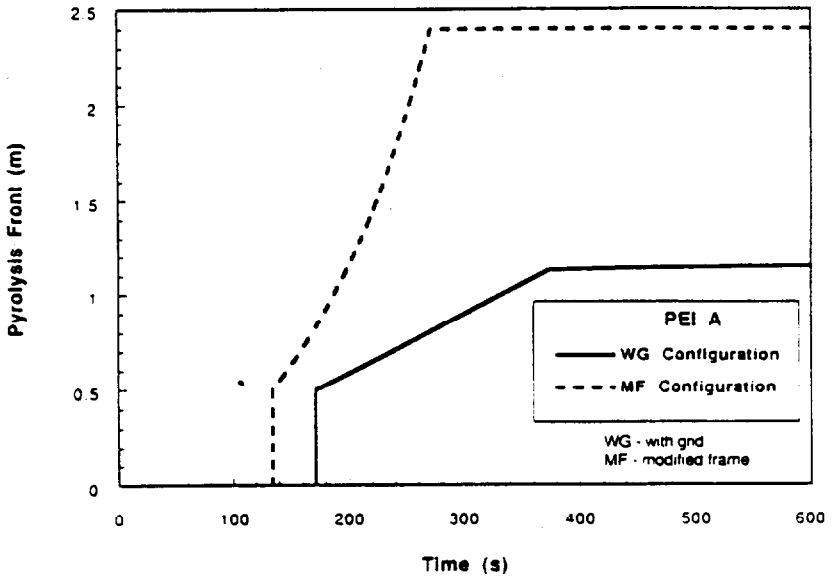

Fig. 14. Comparison of calculated heat release rate for upward flame spread over PEI A using flammability properties measured in the WG and MF configurations.

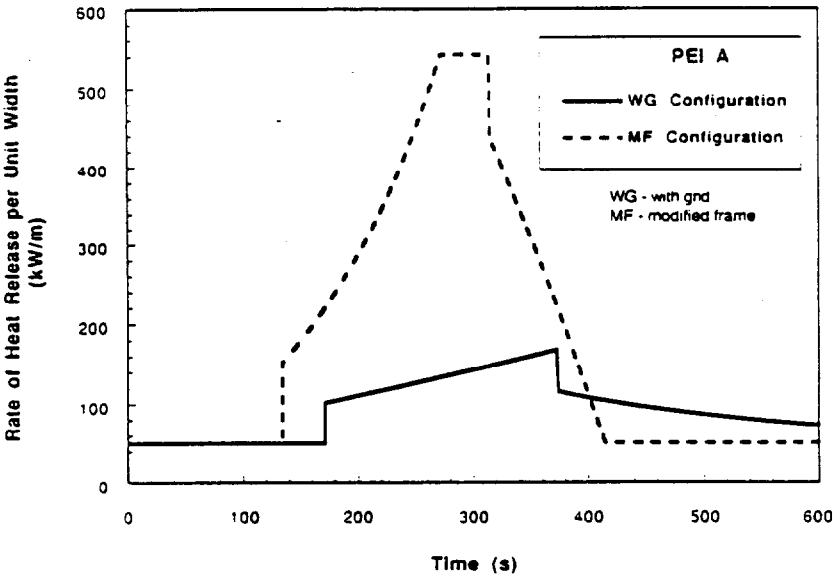

Fig. 15. Comparison of calculated heat release rate for upward flame spread over PEI A using flammability properties measured in the WG and MF configurations.

release rate than those based on the WG configuration. The calculated results for PEI A are shown in Fig. 14 for growth of pyrolysis height and in Fig. 15 for heat release rate. The difference in flammability properties measured by different sample mounting for PEI A significantly affected the flame spread predictions. The calculated pyrolysis front did not reach the top of the wall with the data measured in the WG configuration but it reached the top with the data measured in the MF configuration. The difference in growth of pyrolysis height is reflected in the large difference in calculated heat release rate. Overall peak heat release rate based on the MF configuration is roughly four times larger than that based on the WG configuration. These results clearly show that calculated fire growth rate and overall heat release rate can be very sensitive to the sample mounting configuration in the bench-scale tests.

Although the above calculation has been applied to an artificial case of fire growth (no dripping and melting), it is expected that the predicted results for various fire scenarios by fire growth models would be sensitive to material flammability properties as inputs to the model. At present the measurement of flammability properties for intumescent polymers by a bench-scale test (here, the cone calorimeter and LIFT were used, but by any bench-scale test) needs further study to examine what size of sample and method of mounting are needed to obtain flammability properties applicable to full-scale fire scenarios. It is planned to study flame spread and burning of larger samples of the materials used in this study to observe intumescent characteristics of the char and the flammability properties. This new information should aid the selection of appropriate bench-scale test methodology for determining flammability properties of intumescent polymers.

Although further studies are needed to determine appropriate bench-scale methodology to measure flammability properties of intumescent materials, the approach used in this study demonstrates a great potential to predict the assessment of the fire performance of a polymeric material directly applicable to a wide range of fire scenarios instead of the more traditional approach of using a screening test at a specified set of conditions.

5 CONCLUSIONS

Sample mounting configuration significantly affects the heat release rate behavior of intumescent polymers measured in the cone calorimeter but does not significantly affect integrated flammability properties such as

total heat release, soot yield and effective heat of combustion. A conventional sample mounting method using a screen/grid with a metal container for the cone calorimeter tends to underestimate peak heat release rate and the overall heat release rate curve of intumescent polymers compared with the results obtained in the three different mounting methods used in this study. It does affect flame spread characteristics if a rising char mound is formed well ahead of the advancing flame front. In general, the rank order of the fire performance of the samples appear to be qualitatively the same for any of the four sample mounting configurations used in this study. The test results are useful in evaluating the relative fire performance of the intumescent polymers. However, since the flammability properties are affected by the sample mounting configuration, fire growth predictions derived from these measured properties are also affected by the sample mounting configuration. At present it is not clear what sample mounting condition provides the results applicable to a full-scale fire scenario.

ACKNOWLEDGEMENTS

This work is supported by the Chemical Research Center of General Electric Co. Corporate Research Development at Schenectady, NY. The authors would like to thank Drs Mike MacLaury and John Lupinski of GE for supplying all of the samples used in this study, Mr Randy Shields for operating the cone calorimeter, and Mrs Robin Breese of NIST for her assistance in plotting the figures used in this paper.

REFERENCES

1. Cleary, T. G. & Quintiere, J. G., A framework for utilizing fire property tests. Proceedings of the *Third International Symposium on Fire Safety Science*, (1991) 647–56.
2. Babrauskas, V., Development of the cone calorimeter—A bench-scale heat release rate apparatus based on oxygen consumption. *Fire and Material*, **8** (1984) 81–95.
3. Quintiere, J. G. & Harkleroad, M. T., New concepts for measuring flame spread properties. *ASTM Special Technical Testing Publication 82* (1985) 239–67.
4. Quintiere, J. G. & Harkleroad, M. T., New concepts for measuring flame spread properties. National Bureau of Standards Internal Report, NBSIR 84-2943, 1984.

5. Carslaw, H. S. & Jaeger, J. C., *Conduction of Heat in Solids*. Oxford University Press, Oxford, UK, 1959, p. 72.
6. Quintiere, J. G., The application of flame spread theory to predict material performance. *J. Res. Nat. Bur. Stand.*, **93** (1988) 61–70.
7. Ito, A. & Kashiwagi, T., Characteristics of flame spread over PMMA using holographic interferometry sample orientation effects. *Combust. Flame*, **71** (1988) 189–204.
8. Quintiere, J. G., Harkleroad, M. T. & Hasemi, Y., Wall flames and implications for upward flame spread. *Combust. Sci. Technol.*, **48** (1986) 191–222.